纯铝微弧氧化陶瓷膜组织及耐腐蚀性能

王志平[1]，　孙宇博[1]，　抻英[1]，　刘　佳[1]　蔡　珣[2]
（1. 中国民航大学 理学院，天津　300300；2. 上海交通大学 材料学院，上海　200030）

王志平

摘　要：利用微弧氧化技术，在碱性硅酸盐电解液中对纯铝进行表面改性处理，制备均匀致密的陶瓷膜。利用扫描电子显微镜（SEM）观察氧化陶瓷膜表面形貌及横截面组织结构，利用纳米压入硬度测试仪测量陶瓷膜的显微硬度和杨氏模量的分布，运用电化学方法测量陶瓷膜的耐腐蚀性能。结果表明，铝合金微弧氧化陶瓷膜的表面硬度高达25.3 GPa，纳米硬度和杨氏模量在陶瓷膜的横截面分布相似，从膜基结合处向膜层表面呈下降趋势。从极化曲线中的腐蚀电势和腐蚀电流来看，微弧氧化处理后，纯铝的抗腐蚀能力得到很大的提高。

关键词：铝；微弧氧化；陶瓷膜；耐腐蚀
中图分类号：TG172.6　　文献标识码：A　　文章编号：0253-360X(2008)12-0074-03

0　序　　言

随着现代工业的发展，对材料表面质量要求越来越高，由于铝质材料重量轻、比强度高、耐腐蚀、导电和导热性良好，因此在工业界是极其重要的金属材料；但也有质软，易磨损的弱点，不过随着材料表面改性技术在不断的更新，可以进一步提高铝质材料的表面质量。例如微弧氧化等技术，使铝质材料表面生成质密的陶瓷膜，可以起到耐磨损、耐腐蚀和耐高温的作用[1-3]。

微弧氧化技术又称为微等离子体氧化技术，或阳极火花沉积技术。这是一种在金属及其合金表面通过微等离子体放电进行复杂的电化学、等离子化学和热化学过程，即在金属表面原位生长氧化物陶瓷膜的新技术[4,5]。该技术采用能量密度极高的微等离子弧加热的先进加热方法，基体组织结构不受影响，且工艺不复杂，不造成环境污染，利用此项技术形成的表面膜层与基体的结合力强、膜层硬度高、耐磨性和耐腐蚀性好、抗热震性高、膜层电绝缘好等优点，是一项很有前途的材料表面处理新技术[6]。

1　试验方法

试验材料为纯度99.995%工业纯铝，将材料加工成30 mm×30 mm×170 μm的试样。试样经过丙酮浸湿，超声波清洗后吹干。在交变电流脉冲电源下进行微弧氧化处理。频率为500 Hz；正电流密度为5～20 A/dm^2，正负电流比为1/0.7；正电压为400～600 V，负电压为70～200 V。在微弧氧化进行过程中，保持样品表面电流密度恒定。试验采用的是NaOH和Na_2SO_3混合配比的电解液，在试验过程中，电解液的温度不超过50 ℃。

用美国FEI公司型号为FEI SIRION 200扫描电子显微镜观察陶瓷膜表面形貌及横截面积组织结构。由于陶瓷膜不导电，因此在观察之前要对试样进行喷金处理。采用瑞士CSM公司的型号为S/N6-140纳米压入硬度测试仪，可用于材料的硬度和弹性模量的测试，特别是纳米薄膜的硬度与压入试验。用FISCHER公司的MPOR型涡流测厚仪测出陶瓷膜的厚度为40 μm。

用电化学方法测陶瓷膜的耐腐蚀性能，以极化曲线判断腐蚀性能。腐蚀电势是表征金属（或合金）被腐蚀难易的物理量，腐蚀电势越高，说明该金属（或合金）越难被腐蚀。腐蚀电流是表征金属（或合金）被腐蚀速度快慢的物理量，腐蚀电流越小，腐蚀速度越慢。采用三电极体系，利用PS-168电化学测试系统测定复合材料及微弧氧化膜在质量分数为3.5%的NaCl溶液中的极化曲线来评价膜层的耐腐蚀性能。参比电极为饱和甘汞电极（SCE），辅助电极为铂片。试样经过1 800 s浸泡后从相对于自腐蚀电位的-250 mV扫描到+250 mV，扫描速度为

收稿日期：2008-10-20

0. 167 mV/ s[7] 。

2　试验结果分析

2.1　微弧氧化陶瓷膜形貌

陶瓷膜表面形貌和横截面组织结构如图 1 和图2 所示。

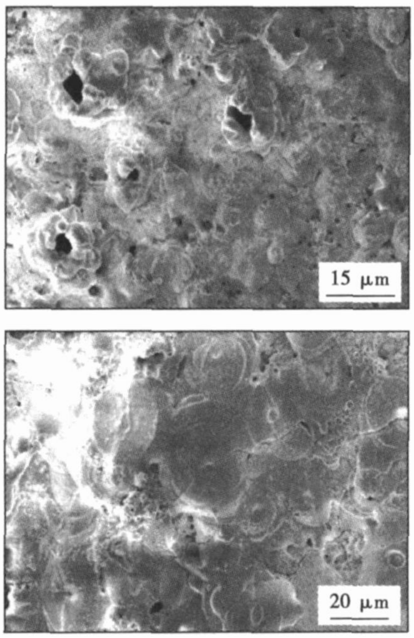

图 1　陶瓷膜表面形貌

Fig 1　Surface morphology of ceramic coating

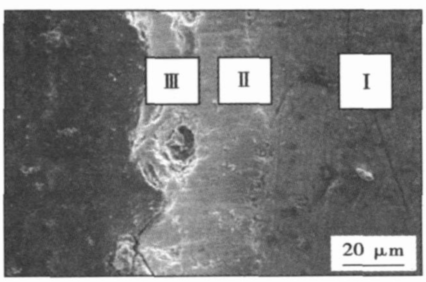

Ⅰ —铝基体; Ⅱ—致密层; Ⅲ—疏松层

图 2　陶瓷膜横截面形貌

Fig. 2　Cross section of ceramic coating

由图 1 可以看出, 陶瓷膜表层残留大量的放电孔洞, 这些放电孔洞是微弧氧化过程中能量最高的部位。在微弧氧化过程中, 由于高电压大电流作用下产生等离子放电, 放电通道内温度高达 2 000 ~ 8 000 K, 压力可达 100 MPa, 击穿表面最薄弱的钝化膜, 在电解液冷却作用下, 迅速冷凝, 形成了火山喷射状的放电通道。孔的周围都是随放电通道中的能量一起迸发出的熔融物质迅速冷凝后的产物。这些熔融物质是在等离子放电条件下, 由电解液中的离子、氧离子与基体结合而形成的。因此微弧氧化陶瓷膜就是在外加电场下, 不断被击穿, 基体被氧化、熔融、凝固、冷却而增厚的。

图是陶瓷膜横截面的 SEM 形貌照片, 陶瓷膜主要由 α-Al_2O_3 和 γ-Al_2O_3 两相组成。外层主要是 γ-Al_2O_3, 由照片可以看出, 组织结构疏松, 并且有很多孔洞存在, 因此称之为疏松层。疏松层的厚度约为 5 ~ 10 μm。内层主要是由刚玉结构的 α-Al_2O_3 相构成, 因此膜层致密, 硬度高, 是防腐蚀、耐磨损的主要工作层, 称之为致密层。致密层的厚度约为 20 ~ 30 μm。疏松层与致密层厚度的比例大致为 1∶2。致密层与基体呈犬牙交错状, 属于冶金结合, 非常牢固。

2.2　陶瓷膜纳米硬度及杨氏模量

纳米压入硬度测试仪是一种先进的能够提供高分辨率连续载荷和位移测量的材料表面力学性能测试仪器。它的定义为, 在压入过程中压痕表面积投影上单位面积所承受的载荷, 它反映样品接触载荷的能力[8] 。本次所有的纳米压入硬度测试仪的试验载荷范围为 0. 1 ~30 mN, 位移准确度为 1 μm, 允许的单层薄膜厚度≥50 nm。图 3 是反映陶瓷膜表面加卸载随位移的曲线。试验中最大载荷和最大压入深度分别为 20 mN, 300 nm。陶瓷膜表面的纳米硬度值和杨氏模量分别为 25. 3 GPa, 117. 5 GPa。

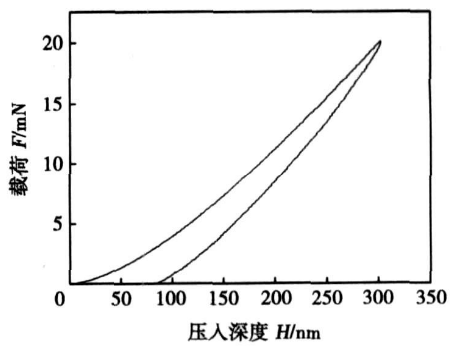

图 3　陶瓷膜表面的纳米加卸载与位移曲线

Fig. 3　Curves of load and unload vs distance

陶瓷膜横截面的纳米硬度和杨氏模量分布情况见图 4。图 4 中横坐标零点位置表示陶瓷膜与基体结合处, 负值坐标表示铝基体距界面处的距离, 正值坐标表示陶瓷膜距界面处的距离。由图 4 可以看出, 陶瓷膜横截面的纳米硬度与杨氏模量分布基本

一致，从铝基体到陶瓷膜表面呈递减趋势，并且最大值均出现在距离界面处 5 ~ 10 μm 附近，分别为 811.49 MPa 和 107.3 GPa。从横截面的 SEM 照片也可以看出，陶瓷膜与基本结合处附近的膜层组织致密，越靠近陶瓷膜表层膜层变得疏松多孔，因此纳米硬度与杨氏模量的分布与陶瓷膜的组织结构是基本一致。

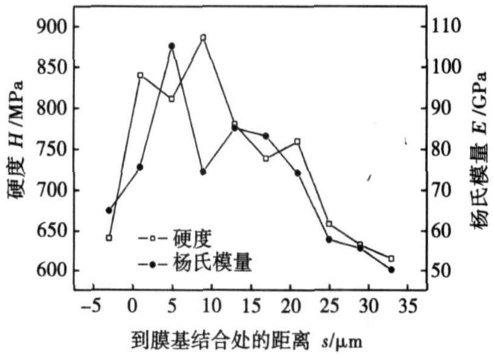

图 4 陶瓷膜横截面的纳米硬度与杨氏模量

Fig. 4 Nano-hardness and Young's modulus of cross section of ceramic coating

2.3 陶瓷膜的耐腐蚀性

铝基材料较铝合金的耐腐蚀性能差，易产生晶间腐蚀，经过微弧氧化处理后，表面产生的陶瓷膜可以有效地提高铝基材料的耐腐蚀性能[9]。图 5 是基体与微弧氧化陶瓷膜在质量分数为 3.5%的 NaCl 溶液中电化学测量的极化曲线结果。从极化曲线中可以得到样品的腐蚀电势和腐蚀电流密度。未经微弧氧化处理的样品经电化学测试后，腐蚀电势为 −0.662 V，腐蚀电流密度为 4.4145×10^{-7} A/cm^2；而经过铝微弧氧化处理后，表面生成一层致密陶瓷膜后，腐蚀电势明显得到提高，上升到 −0.238 V，腐蚀电势提高了 0.4 V 电位，极大地提高了样品的抗腐蚀能力；同时腐蚀电流密度也达到了 8.919×10^{-10} A/cm^2，腐蚀电流降低了 3 个数量级，进一步减少了样品被腐蚀的速度。

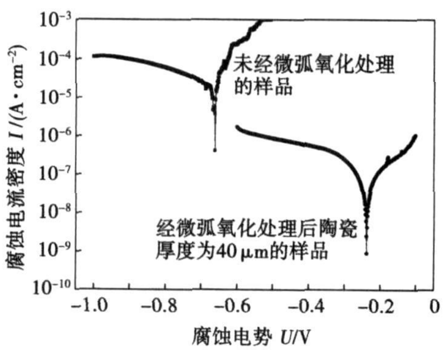

图 5 基体与涂覆微弧氧化膜试样的极化曲线

Fig. 5 Polarization curves of substrate and ceramic coating

3 结 论

（1）纯铝微弧氧化陶瓷膜有疏松层和致密层两层结构，膜层硬度高，可以有效地保护基体材料。

（2）陶瓷膜横截面的纳米硬度和杨氏模量分布规律基本相似，在界面处硬度和杨氏模量达到最大值，沿着膜层表面的方向，硬度和杨氏模量逐渐减小。

（3）微弧氧化陶瓷膜使腐蚀电势提高了 0.4 V 电位，腐蚀电流密度减小了 3 个数量级，陶瓷膜可以有效的提高纯铝的耐腐蚀性能。

参考文献：

[1] Sundararajan G, Krishna L R. Mechanisms underlying the formation of thick alumina coatings through the MAO coating technology[J]. Surface and Coatings Technology, 2003, 167: 269−277.

[2] 沈德久，王玉林，卢立红，等. 铝合金表面微弧氧化自润滑陶瓷覆层[J]. 材料保护，2000，33(5)：51−52.

[3] 辛铁柱，赵万生，刘晋春. 铝合金表面微弧氧化陶瓷膜的摩擦学性能及微观结构研究[J]. 航天制造技术，2005(4)：5−8.

[4] Rakoch A G, Khokhlov V V, Bautin V A, *et al*. Model concepts on the mechanism of microarc oxidation of metal materials and the control over this process[J]. Protection of Metals, 2006, 42(2): 158−169.

[5] 滕 敏，赫晓东，李 垚. 铝合金等离子体微弧氧化陶瓷层组织与性能研究[J]. 航空材料学报，2004，24(6)：47−49.

[6] 薛文斌，吴晓玲，施修龄，等. SiC_p/2024 铝基复合材料表面微弧氧化膜组织结构及其耐蚀性[J]. 复合材料学报，2006，23(6)：98−102.

[7] Xue Wenbin, Wang Chao, Tian Hua, *et al*. Corrosion behaviors and galvanic studies of microarc oxidation films on Al-Zn-Mg-Cu alloy[J]. Surface and Coatings Technology, 2007, 201(2): 8695−8701.

[8] 张泰华，杨业敏. 纳米硬度技术在表面工程力学性能检测中的应用[J]. 中国机械工程，2002，13(24)：2148−2150.

[9] 辛世刚，宋力昕，赵荣根，等. 铝基复合材料微弧氧化陶瓷膜的组成与性能[J]. 无机材料学报，2006，21(1)：223−229.

作者简介：王志平，男，1963 年出生，教授。主要研究方向为热喷涂及焊接技术。发表论文 20 余篇。

Email：dingkunying@126.com

010051, China; 2. Baotou North Engineering Development Co., Ltd, Baotou 014033, China). p57—60

Abstract: The 7A52 aluminum alloys of 40mm in thickness were welded by using Twin-wire gas shielded arc welding (DWGSAW) with ER5356 filler, and the microstructure of the weld seam was analyzed. Meanwhile, according to the actual application environment, the base metal and the weld seam were studied in 3.5% NaCl solution after welding. Results show that the microstructure of the seam welded by DWGSAW is composed of α(Al)+β($MgZn_2$), which the crystal grain is compact and petty, and the center of the weld is equiaxed grain. The corrosion resistance of 7A52 aluminum alloy is liable to pitting corrosion in humid environment containing chloride iron. However, a thin and condense aluminum oxide film is formed on the corroded surface, which is beneficial to increasing the corrosion resistance of the 7A52 aluminum alloy. The corrosion resistance of the weld seam is better and the pitting corrosion is rare on the corroded surface.

Key words: 7A52 aluminum alloy; double-wire gas shielded arc welding; microstructure; corrosion resistance

Solidification crack of SnAgCu lead-free solder joint DONG Wenxing, SHI Yaowu, XIA Zhidong, LEI Yongping, GUO Fu, LI Xiaoyan (School of Materials Science & Engineering, Beijing University of Technology, Beijing 100124, China). p61—63, 68

Abstract: In order to investigate solidification crack of SnAgCu solder joint on the print circuit board (PCB), solidification cracks during solidification are regenerated, the process of the solidification crack formation on the designed specimen is simulated, and the effect of the small element additions on the solidification crack formation of SnAgCu solder joint is researched. Experimental results indicate that some solidification micro-cracks exist significantly on the mini SnAgCu solder joint. The solidification crack susceptibility of Sn-Ag-Cu solder alloy is evaluated by the total crack length of the solder joint, adding trace amounts of Ni and Ce element can depress the solidification crack formation of the solder joints, but adding P element can aggravate the solidification crack formation of SAC305 solder joint and make the crack length evidently increase.

Key words: lead-free solder; SnAgCu solder; solidification crack

Algorithm of weld seam feature detection for remote welding ZHAO Huihui, LIANG Zhimin, GAO Hongming, WU Lin (State Key Laboratory of Advanced Welding Production Technology, Harbin Institute of Technology, Harbin 150001, China). p64—68

Abstract: An algorithm of weld seam feature detection was presented, which was applied to stereo matching of stereo vision system for remote welding. Firstly, the bottom-hat transformation in grey-scale morphology was used to preprocess the image, making the weld seam section more distinctive, and Canny edge detection and close operation were employed to obtain a pixel level closed edge of weld seam; secondly, the edge data was filtered according to continuity and limited width of the weld seam edge; finally, the sub-pixel weld seam edge data was gained by fitting a cubic smoothing spline to the filtered edge data. With the detected sub-pixel weld seam, stereo matching and 3D reconstruction experiments were performed. The results show that the algorithm is rapid, exact and robust to noises.

Key words: remote welding; 3D reconstruction; stereo vision; weld seam feature detection

Effect of relative position of laser beam and arc on formation of weld in laser-MIG hybrid welding GAO Zhiguo, HUANG Jian, LI Yaling, WU Yixiong (Shanghai Key Laboratory of Materials Laser Processing and Modification, Shanghai Jiaotong University, Shanghai 200240, China). p69—73

Abstract: In order to weld high reflectivity aluminum alloy 5083H116 by laser-MIG hybrid welding process, the effects of the front and behind relative position of laser beam and arc on the formation of weld were analyzed. The laser beam incidence angel will seriously affect the weld formation both surface and inside corresponding to different formation mechanism. When the laser beam is in front of the arc in the welding direction, the weld surface is full uniform. While the arc is in front of the laser beam in the welding direction, the inclined trench will appear on the weld surface. With the help of EDX and micro hardness analysis, the Mg content shows a gradual increase from the weld upside surface to the underside surface, but the weld hardness is slight difference. The weld hardness of upside is less than that of underside for the laser beam in front of the arc in the welding direction; the weld hardness of upside is higher than that of underside for the arc in front of laser beam in the welding direction. Meanwhile, there is the black substance on the weld surface after welding, and it is confirmed as oxide of aluminum and magnesium by the EDX.

Key words: aluminum alloy; weld formation; laser-MIG hybrid welding; laser incidence angle

Structure and electrochemistry corrosion behaviors of microarc oxidation on aluminum WANG Zhiping[1], SUN Yubo[1], DING Kunying[1], LIU Jia[1], CAI Xun[2] (1. College of Sciences, Civil Aviation University of China, Tianjin 300300, China; 2. School of Materials Science and Engineering, Shanghai Jiaotong University, Shanghai 200240, China). p74—76

Abstract: The thick, dense and ultra-hard ceramic coating was obtained on the aluminum surface in a silicate electrolyte by microarc oxidation. The surface morphology and cross section of ceramic coating were observed by SEM, the hardness and Young's modulus of ceramic coating were estimated by nano-hardness tester, and the electrochemistry corrosion behaviors of ceramic coating were evaluated using polarization curves. The results show that the highest surface hardness of ceramic surface coating is 25.3 GPa; the hardness and Young's modulus of cross section of coating distribute similarly, both of them decrease from interface to surface of the coating; from the results of electrochemistry, microarc oxidation is effective method to form an anti-corrosion protective film on aluminum.

Key words: aluminum; microarc oxidation; ceramic coating; electrochemistry corrosion behaviors